Article

Diversity in Zooplankton and Sympagic Biota during a Period of Rapid Sea Ice Change in Terra Nova Bay, Ross Sea, Antarctica

Antonia Granata [1], Christine K. Weldrick [2], Andrea Bergamasco [3], Maria Saggiomo [4], Marco Grillo [5,6], Alessandro Bergamasco [3,*], Kerrie M. Swadling [2,7,†] and Letterio Guglielmo [4,†]

[1] Department of Chemical, Biological, Pharmaceutical and Environmental Sciences (ChiBioFarAm), University of Messina, 98166 Messina, Italy; antonia.granata@unime.it
[2] Australian Antarctic Program Partnership, University of Tasmania, Hobart 7001, Australia; christine.weldrick@utas.edu.au (C.K.W.); k.swadling@utas.edu.au (K.M.S.)
[3] Institute of Marine Sciences, National Research Council (CNR-ISMAR), Section of Venice, 30122 Venice, Italy; andrea.bergamasco.cnr@gmail.com
[4] Stazione Zoologica Anton Dohrn, 80121 Napoli, Italy; maria.saggiomo@szn.it (M.S.); letterio.guglielmo@szn.it (L.G.)
[5] Department of Physical Sciences, Earth and Environment (DSFTA), University of Siena, 53100 Siena, Italy; grillomarco94@gmail.com
[6] Italian National Antarctic Museum (MNA, Section of Genoa), University of Genoa, 16132 Genoa, Italy
[7] Institute for Marine and Antarctic Studies, University of Tasmania, Hobart 7001, Australia
* Correspondence: alessandro.bergamasco@ve.ismar.cnr.it
† These authors jointly supervised this work: Swadling Kerrie and Guglielmo Letterio.

Abstract: Sea ice is a major driver of biological activity in the Southern Ocean. Its cycle of growth and decay determines life history traits; food web interactions; and populations of many small, ice-associated organisms. The regional ocean modelling system (ROMS) for sea ice in the western Ross Sea has highlighted two modes of sea ice duration: fast-melting years when water temperature warms quickly in early spring and sea ice melts out in mid-November, and slow-melting years when water temperature remains below 0 °C and sea ice persists through most of December. Ice-associated and pelagic biota in Terra Nova Bay, Ross Sea, were studied intensively over a 3-week period in November 1997 as part of the PIPEX (Pack-Ice Plankton Experiment) campaign. The sea ice environment in November 1997 exhibited features of a slow-melting year, and the ice cover measured 0.65 m in late November. Phytoplankton abundance and diversity increased in the second half of November, concomitant with warming air and water temperatures, melting sea ice and progressive deepening of a still weak pycnocline. Water column phytoplankton was dominated by planktonic species, both in abundance and diversity, although there was also some input from benthic species. Pelagic zooplankton were typical of a nearshore Antarctic system, with the cyclopoid copepod *Oithona similis* representing at least 90% of total abundance. There was an increase in numbers coinciding with the period of ice thinning. Conversely, ice-associated species such as the calanoid copepods *Stephos longipes* and *Paralabidocera antarctica* decreased over time and were found in low numbers once the water temperatures increased. Stratified sampling under the sea ice, to 20 m, revealed that *P. antarctica* was mainly found in close association with the under-ice surface, while *S. longipes*, *O. similis*, and the calanoid copepod *Metridia gerlachei* were dispersed more evenly.

Keywords: diatoms; copepods; spring sea ice; multinet; Southern Ocean

1. Introduction

Sea ice surrounding the Antarctic continent varies in extent from 3.1×10^6 km^2 in February to a maximum of 18.5×10^6 km^2 in September [1,2], making it one of the largest and most dynamic ecosystems on Earth [3]. About 5 to 25% of the marine primary production in the Southern Ocean is associated with sea ice, with algae inhabiting the internal systems of pores, brine channels and crannies ([4,5] and references therein). Ice

algal standing stocks (algal biomass) and primary productivity may reach values as high as 400 mg Chla m^{-2} and 1 g C m^{-2} d^{-1}, respectively [6–9], providing a rich food source for ice-associated fauna, along with pelagic and benthic organisms [10–13]. During late spring to early summer, this biomass is released into the water column after ice melting [14,15] and can fuel both the pelagic and benthic coastal environments by releasing large amounts of bioavailable organic carbon [16,17].

Polar shelf regions are important sites for water mass formation and transformation. Shelf seawater is strongly influenced by heat and evaporation fluxes between the ocean, the ice, the sea ice, and the atmosphere, as well as exchange with the open ocean. In the Ross Sea, circumpolar deep water (CDW) intrudes onto the shelf, undergoes mixing, and contributes to the transformation of the Ross Sea Shelf Water, characterised as T $\approx$ −2.0 °C and S = 34.4 to 34.8 [18,19]. During spring, close to the pack-ice borders, local mixing is enhanced by recurrent events of lateral advection of fresher water at the melting-point temperature due to the ongoing melting of the rear pack interacting with coastal recirculation and progressive seasonal surface warming [20,21]. Ross Sea Shelf Water is mainly formed during winter when there is large heat loss to the atmosphere. In the polynya areas, during sea ice freezing and rapid removal by katabatic winds, local brine rejection increases the salinity, producing a subsequent convective sinking that fills up deeper basins such as those near the Drygalski Ice Tongue [22,23].

Sea ice melting influences physico-chemical characteristics and biological processes of the water column [24,25], and it triggers mechanisms sustaining both the pelagic and benthic food webs [26–32]. Strong interannual variability of sea ice covering and thickness is observed also from studies based on remote sensing data (see [1,2] and references therein), pointing out that seasonal cycle of sea ice is characterised by slow growth and fast melt season, strongly modulated by regional scale processes. In the last decade, several studies have shown that ice formation–melting processes are responsible for changes in quantity and composition of microbial and planktonic communities [8,31,33–36].

Sea ice harbours a range of organisms and acts as a refuge, breeding, feeding and nursery ground for the early developmental stages and juveniles of many species. The pelagic silverfish *Pleuragramma antarcticum* spawns just beneath sea ice, and a considerable quantity of eggs and first larval stages accumulate within the bottom ice [37,38]. Sea ice biota includes a variety of micro-organisms, such as heterotrophic bacteria [39,40], micro-algae, heterotrophic protozoa (e.g., flagellates, ciliates, foraminiferans), and metazoans (e.g., copepods and turbellarians, [8,41–45]), living within the ice (sympagic organisms), as well as larger animals living in the lowest part of the sea ice and at the sea ice–water interface [41]. Copepods and turbellarians are the most abundant members of the sympagic meiofauna [46–50]. Two species, *Oithona similis* and *Metridia gerlachei*, exhibit a strong affinity with the pelagic habitat in Terra Nova Bay, whereas the dominant copepod species of the Antarctic sea ice assemblages are the harpacticoids *Drescheriella glacialis* and *Harpacticus furcifer* and the calanoids *Stephos longipes* and *Paralabidocera antarctica* [45,51–56], which inhabit the ice–seawater interface for part (*S. longipes*) or the whole (*P. antarctica*) of their life cycles. Several studies of the distribution and production of planktonic communities in the Ross Sea have reported high biological production occurring from spring to early summer, both offshore and in coastal areas [57]. In particular, in the south-western coastal area, successive algal blooms have been observed from early spring until autumn, both in the sympagic and pelagic realms [58].

The quantifying of energetic fluxes among the biota, pack ice (the bottom-ice community), platelet layer, and free sea ice water are of scientific interest for understanding the high Antarctic carbon cycle. However, quantitative sampling of plankton communities from ice-covered waters presents many technical and logistic difficulties as it is hard to sample this harsh under-ice ecosystem using conventional samplers. The boundary layer between the sea ice and the underlying water gets disturbed during coring and the ice cover largely precludes horizontal and oblique net tows, although vertical tows for under-ice sampling are possible through ice holes [59]. We developed a sampling system with

horizontal displacement capability, the MicroNESS [60], which is deployable through an ice hole and able to sample zooplankton at different depths beneath the ice.

The aims of this study were to: (a) describe the composition and the structure of the ice algae and ice-associated copepods in the free water under sea ice in Terra Nova Bay during a period of springtime melting, (b) understand how biotic parameters change over a short time period when ice melting starts, (c) determine whether ice-associated copepods are related to sea ice algae released by ice melting, and (d) contribute to the knowledge of the life cycle of some key pelagic (*Oithona similis* and *Metridia gerlachei*) and ice-associated copepod species (*Stephos longipes* and *Paralabidocera antarctica*).

2. Materials and Methods

Within the framework of the PIPEX (Pack-Ice Plankton Experiment) 1997-98 project, funded by the PNRA (Programma Nazionale di Ricerche in Antartide), a multidisciplinary cruise was carried out during November 1997 in Terra Nova Bay, Western Ross Sea (74°41.72′ S, 164°11.63′ E, Figure 1). Temporal variation in under-ice microalgal sedimentation and plankton dynamics were followed throughout a period of rapid changes in water temperature and sea ice thickness.
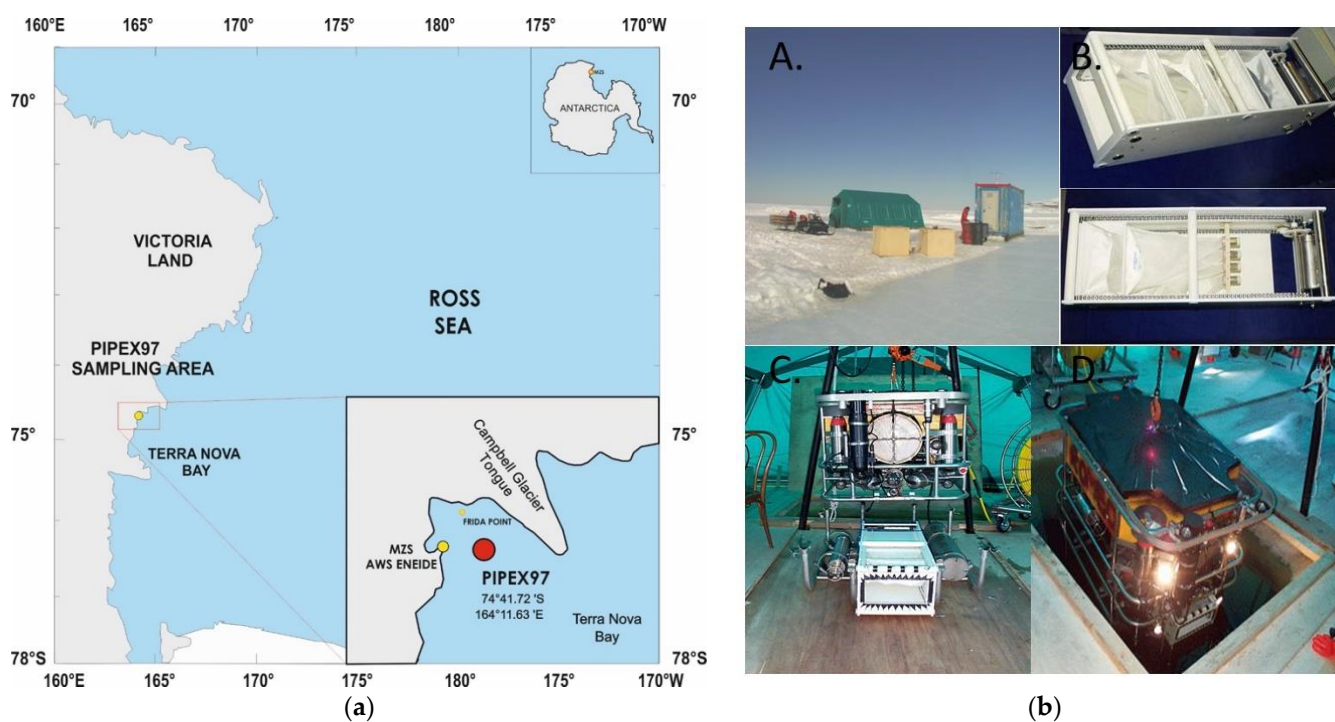
Figure 1. The field settings at the PIPEX 97 project sampling area, Terra Nova Bay, Antarctica, 1997. (**a**) The positions of the meteorological (ENEIDE) and the oceanographic (FRIDA) stations. (**b**) The biological station and the details inside the tent during field activities: (A) the sampling area on the pack-ice; (B) top view of the MicroNESS and position of the 4 sampling nets; (C) the attachment of MicroNESS to the ROMEO structure; (D) the deployment of the system through the hole in the ice.

2.1. The Sea Ice Environment

To place the PIPEX cruise conditions in the context of long-term interannual variability in the ecosystem, a ROMS (Regional Ocean Modelling System) circulation model of the entire Ross Sea was used to describe how sea ice thickness responds to changing water temperature. The model gives the opportunity to explore in more detail in the time window of interest the short-term local behaviour of sea ice features and the interplay with the water column characteristics. Output from ROMS simulations [61] made available by the authors was obtained by forcing the system with real boundary conditions (ERA-40), spanning a time window domain of 15 years (from 1999 to 2013). A grid cell of 5×5 km^2, covering the

PIPEX sampling stations, was identified, and then the time series of modelled variables along the water column (temperature, salinity) for late October to end of January over the 15 year period was extracted along with ice-related surface variables (ice thickness and percentage of ice-covered area in the selected grid cell). The meteorological data were collected at the ENEIDE automatic weather station (Figure 1a; Argos ID 7353, lat 74° 42′ S; lon 164° 06′ E, height = 90 m). Vertical CTD profiles up to 250 m depth were collected at FRIDA point during the PIPEX cruise by a SBE 911 CTD.

2.2. Sampling Procedure

The vertical distribution of microalgae and copepods in the water column under the sea ice were studied by stratified sampling with the MicroNESS, a zooplankton multinet sampler [60]. MicroNESS is a small plankton sampling device that enables the horizontal hauling in the water layer close to the undisturbed pack ice (i.e., far from ice borders or sources of light such as artificial holes) to capture a wide range of plankton specimens living just below the ice pack itself. It consists of a rectangular main frame (length 810 mm, height 280 mm, width 340 mm) that houses four conical plankton nets (130 × 270 mm in mouth, 450 mm in length, 0.10 mm mesh size; Figure 1b). On the basis of previous observations a mesh size of 100 μm on the MicroNESS exhibits optimal catching capabilities in the size range 100–600 μm, even though it is capable of catching specimens up to 5 mm [60]. This mesh size has been proved to be suitable for both qualitative studies of the phytoplankton community and semi-quantitative evaluation of zooplankton in the under-ice polar environment. The MicroNESS was mounted on a ROV (remotely operated vehicle) that was immersed under the pack-ice, which was 130 cm in thickness, through an artificial rectangular hole (150 × 200 cm). During the horizontal tows, the multiple opening and closing net was totally controlled electronically.

Samples were collected from seven discrete layers, from ≈2 m below the sea ice to 20 m (3.5, 4.5, 5.0, 6.0, 7.0, 10, and 20 m; Figure S1) in an area where the water depth ranged between 400 and 450 m. Zooplankton were collected approximately 250 m from the artificial hole to avoid any environmental alteration, e.g., increased light. The ROV was equipped with a multiparametric probe (IM5196) to measure, simultaneously to the sampling, temperature (°C), conductibility, depth (m), oxygen, fluorescence, and turbidity.

During the study period (17–29 November 1997), a total of 96 plankton samples were collected (Table S1). From November 19, two samplings were performed daily with a 7 h interval between them (10:00 h and 17:00 h). Each MicroNESS net was towed at each depth layer for about 14 minutes. The volume of seawater filtered was calculated with a General Oceanics flowmeter, mounted in the mouth of one net, which monitored in real time the relative speed of the ROV against the water speed. The efficiency ratio was maintained as high as possible on the basis of a cruise speed at max 0.25 m s^{-1}. Filtration efficiency was calculated by dividing meter readings from the front meter versus the ROV speedometer. Filtration efficiency of around 100% should help to eliminate the acceleration fronts that warn organisms of the nets' approach, thus reducing avoidance by the more motile specimens. Each collected sample (500 mL) was split into two subsamples of 250 mL, for zooplankton and phytoplankton analysis, and preserved in 4% and 2% buffered formalin-seawater solution, respectively. Unfortunately, some of the phytoplankton samples were damaged and lost during transportation.

2.3. Laboratory Procedures

Phytoplankton

The phytoplankton species composition and cell abundance were determined following the Utermöhl method [62], according to which at least 200 cells were counted per sample, using a Zeiss Axiophot inverted microscope (Carl Zeiss, Oberkochen, Germany) operating with phase contrast optics at 400× magnification [63]. Phytoplankton taxa were identified to the lowest possible taxonomic rank [64–67]. Questionable identifications were resolved by pooling similar specimens together in higher-rank taxonomic groups.

Zooplankton

In the laboratory, the total zooplankton sample was examined, and copepods were sorted (by species, sex, development stages) and counted. Depending on the abundance of organisms, the whole sample, or an aliquot of 1/2 to 1/10 subsamples was examined. The identification of the specimens and their developmental stages, when possible, was carried out according to [68–74]. Differences between *S. longipes* and *P. antarctica* nauplii, mainly based on the second antennular maxilliped, and the caudal armature, have been useful for distinguishing between the two species [74]. Body length was measured from the anterior to posterior end of the naupliar body, and from the base of the rostrum to the posterior edge of the caudal rami in copepodites. Specimens of each developmental stage were mounted on a glass slide and examined under an optical microscope at 40× magnification. The count of each developmental stage was converted to individual numbers per unit volume of water. Mean naupliar stage for key copepod species was calculated using the abundance data, according to the equation of Huntley and Escritor (1991)

$$[S] = (NnI + 2NnII + \ldots + 6NnVI)/CN \tag{1}$$

where NnI, NnII, ... NnVI = number of specimens of naupliar stages NI, NII, ... NVI, and CN = the sum of all individuals [75].

Statistical analyses of the data were performed with the Statgraphics package [76]. To test for differences between and within groups of data (dates, depth of tow, etc.), ANOVA together with post hoc tests was used, following suitable transformation to ensure homogeneity of the variances. Patterns in the phytoplankton community were explored using Primer v.7 (diversity and similarity among communities) and the R-package Vegan, version 2.2-1 [77]. To evaluate the sampling effort, species accumulation plots were compared and the extrapolated species richness in the species pool was calculated, giving an estimate of the number of unobserved species using the R-packed Vegan version 2.2-1 [77].

3. Results

3.1. Meteorology and Oceanography

The meteorological data collected at ENEIDE in Terra Nova Bay from late October to late November 1997 are shown in Figure 2. The air temperature remained well below $-10\,°C$ until early November, when an episode of strong wind marked the beginning of spring, as indicated by the general increase in insolation maxima (up to 500 Wm^{-2}) and daily average air temperatures (from $-5.1\,°C$ on Nov 5 to $+3.4\,°C$ on Nov 21). At the end of November, air temperature decreased abruptly, from daily averages of $+1.2\,°C$ (22 November) to below $-5.0\,°C$ (29 November).

Temperature and salinity measured during November at FRIDA point (Figure 1; 74°41.725 S; 164°11.633 E), which is close to the PIPEX field site, are shown in the T-S diagram of Figure 3a. Two main oceanographic features are highlighted: (1) the presence of water masses with low salinity, due to ice-melting, entering the site at ≈25 m depth, and (2) the process of mixing on the shelf leading to the formation of Antarctic Shelf Water (T = $-1.9\,°C$, S = 34.75). Focusing on the vertical profiles in terms of potential density anomaly, at the beginning of the month, the water column exhibited a vertically homogenous temperature close to the freezing point and density anomaly equal to 28.01 kg m^{-3}. After that, the density in the upper 10 m thick layer decreased below 28 kg m^{-3} due to the joint effect of weak warming and dilution, which produced a mixed layer down to about 40 m depth. These processes proceeded very slowly to form a small vertical density gradient. Towards the end of the period, the surface warming became stronger ($+0.2\,°C$), and the pycnocline, though not well defined, progressively deepened, possibly facilitating the ingression of lateral fresher tongues. Density in the upper 10 m thick layer further decreased to 27.94 kg m^{-3}, fostered by the pack-ice melting that induced salinity minima of ≈34.7 at 5 to 10 m depth and generated a mixing layer from 10 to 30 m depth.
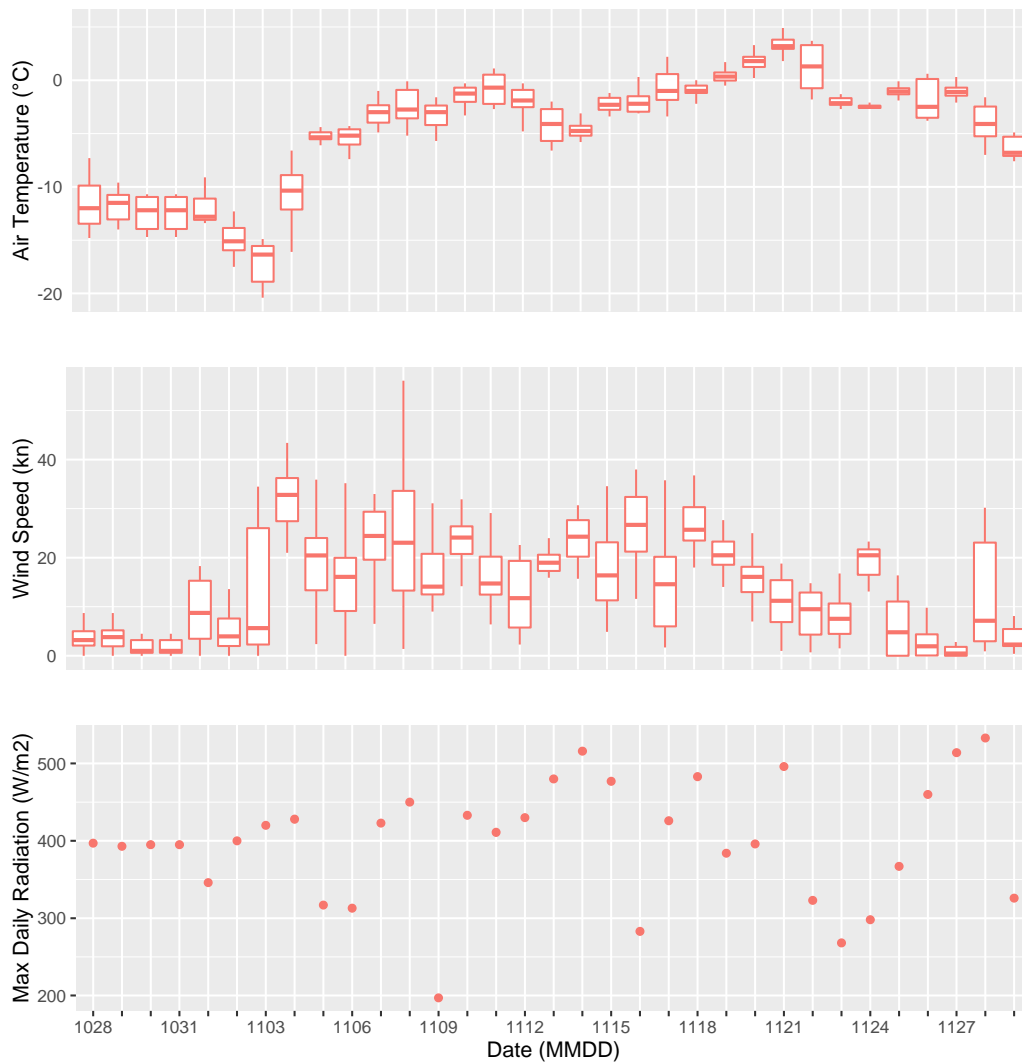
Figure 2. Meteorological data, November 1997, ENEIDE Station. Note the different trend of air temperature between week I (14–21 November) and week II (22–29 November).
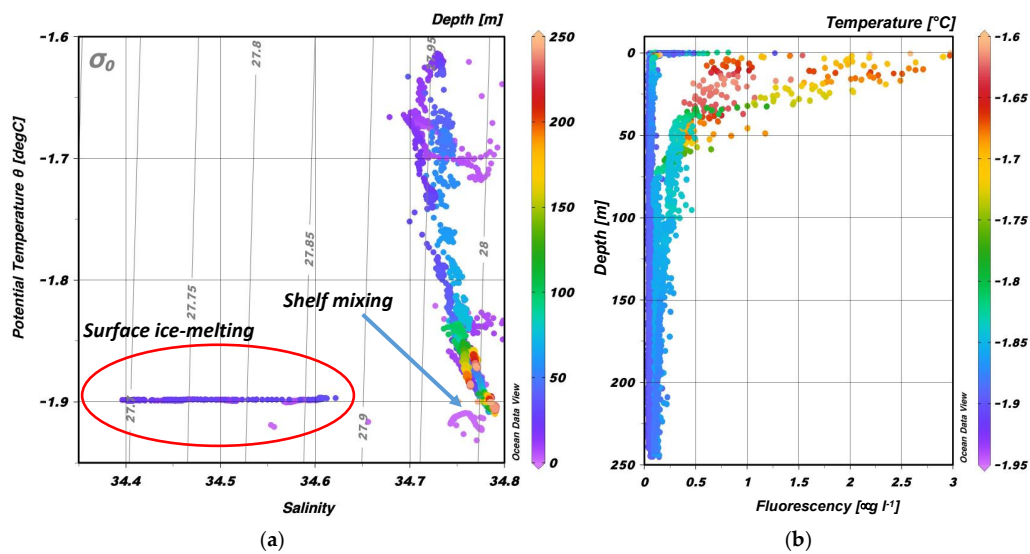
Figure 3. Oceanographical data, FRIDA Station. (**a**) T-S diagram. (**b**) Vertical profiles of fluorescence (dates: 7, 13, 17, 21, 26, and 28 November).

A uniform background fluorescence of about 0.1 ug l^{-1} was present throughout the water column when the temperature was close to the freezing point ($-1.86\,^\circ$C) during the first week of the campaign (Figure 3b). An increase in fluorescence was observed during the second week of sampling, when the surface temperature increased. At the very end of November, warmer temperatures led to a strong increase in biological activity, as highlighted by the fluorescence profiles that increased to 10-to-20 times the background values in the mixed layer.

During the first half of November, temperature varied little throughout the water column (Figure 4, upper left panel); averages remained close to the freezing point ($-1.86\,^\circ$C), with only a light signal of surface warming. Salinity exhibited strong fluctuations in the uppermost 20 m due to ongoing ice melting (Figure 4, upper right panel); averages ranged around 34.6–34.7, and episodes of surface intrusion of fresher water, possibly from lateral advection, were observed. During the second half of November, surface warming increased, and the expected water mixing on the shelf dominated, with noticeable effects down to 50 m depth (Figure 4, upper left panel); average temperatures within the layers sampled by MicroNESS were $\approx-1.5\,^\circ$C, with salinity $\approx$34.8 (Figure 4, upper right panel). In the later period, no evident effects of fresher inputs were observed.
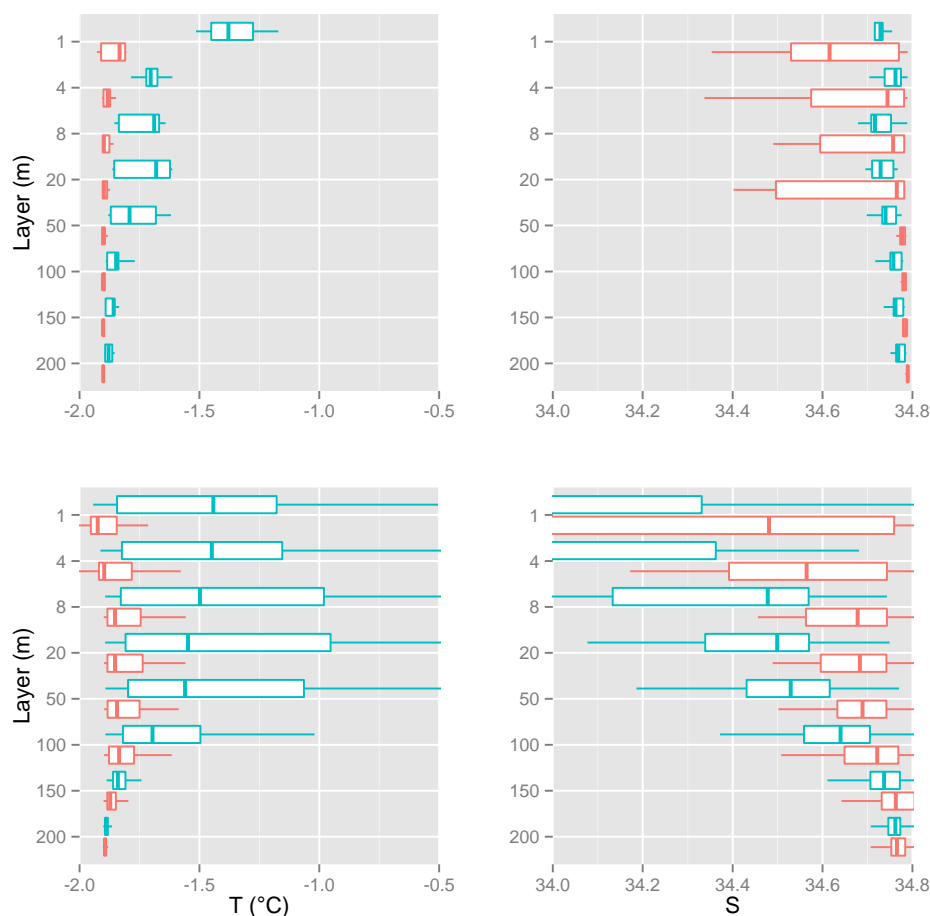
Figure 4. Upper panels: Field temperature (**left**) and salinity (**right**) measured at FRIDA station. Lower panels: Temperature (**left**) and salinity (**right**) modelled in the Terra Nova Bay area. Red boxes refer to the first half of November; green boxes refer to the second half of November.

The output from the ROMS modelling is shown in the lower panels on the same figure (Figure 4, lower panels, T and S); to facilitate comparison, the values were binned into the same vertical depth strata used for the measured profiles. As expected, the variability in model output appears larger than (but consistent with) measured variability, since the modelled data integrated both the climatic fluctuations of 15 years and the spatial

conditions of a 5 × 5 km² cell. The variability was more pronounced in the second half of November for both T and S. In particular, within the 20 m thick uppermost layer and below 150 m depth, the modelled thermal structure reflected the trend shown in the PIPEX field data, while the intermediate layer (50–150 m) exhibited more dynamic behaviour. For salinity, during the first half of November, the observed ranges were well represented within the modelled variability, whereas in the second part of the month the uppermost layers appeared to be more dynamic and dominated by ice-related processes, leading to an excess of freshening.

Comparisons, based on the ROMS, of simulated vs. measured surface water temperature and simulated trend in ice thickness at the PIPEX station from mid-October to the end of January are shown in Figure 5.
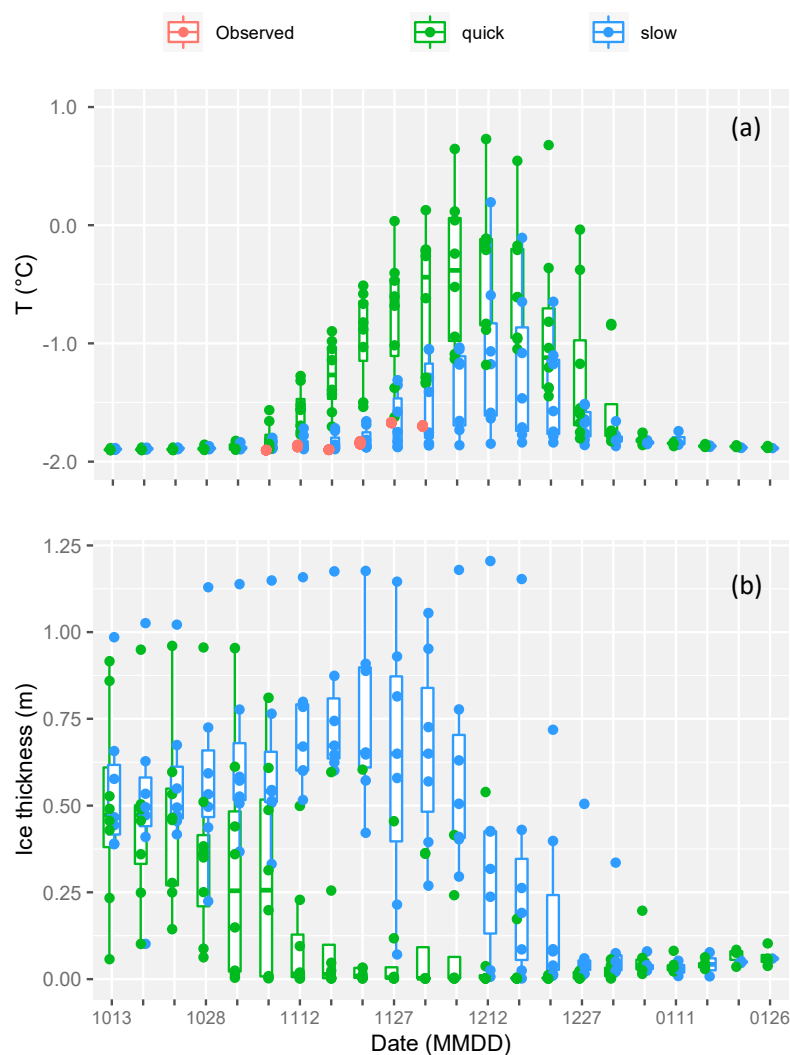
Figure 5. (**a**) Comparisons of simulated vs. measured surface water temperature. (**b**) Simulated trend of ice thickness at the PIPEX station from mid-October to end of January. Years are classified as quick/slow-melting. The observed temperature measured with the CTD in the 5–8 m layer (in red) are representative of a typical year of slow (or delayed) melting in the area. The date is coded as MMDD, from 13 October (1013) to 26 January (0126).

The surface temperature of the uppermost 8 m from the end of October to the beginning of December over the considered 15 years were grouped into 5-day bins and then classified according to the typical thermal behaviour (corresponding to the melting starting phase) (Figure 5a). Before 7 November, there were no significant differences between the years. The surface temperature was stable around the freezing point (−1.86 °C), with only minor

fluctuations. From this date onward, the temperatures diverged: the fast-melting-years (green points) showed an evident warming, despite the variability, whereas for the slow-melting-years (blue points), melting was delayed by two to three weeks. Surface water temperatures measured during the PIPEX cruise (1997, red dots) fall within the expected variability of a typical year of slow (or delayed) melting in the Terra Nova Bay area.

The consequences of these two warming scenarios for sea ice thickness around the PIPEX sampling station, as simulated by ROMS, are shown in Figure 5b. Again, fast-/slow-melting years are shown in green/blue, respectively. On the basis of ROMS, from mid-October, the ice thickness remained around 40–50 cm, regardless of the melting type. In the following month (mid-October to mid-November), a gap began to appear between the two types of melting and progressively widened in the second half of November (from 12 Nov) up to the beginning of December (7–12 December) when there was the greatest difference. Then, from mid-December onwards, the boxes were again almost overlapping and indicated a thin ice sheet of about 0–10 cm at the beginning of January, indicating an almost completed melting period.

3.2. Phytoplankton Community

The phytoplankton community was dominated by diatoms, whose abundance reached almost 100% of total species abundance on most occasions. Diatom abundance generally increased over time, with minima occurring at the beginning of the first week of sampling (10^5 cell l^{-1}, daily average) and maxima around the end of the sampling period (10^7 cell l^{-1}, daily average). The diatom community (Table 1) exhibited an overall richness of 32 taxa and was represented by both benthic (11) and pelagic (21) genera/species.

Pelagic species dominated the phytoplankton community, and the highest abundance was observed on Nov 26 (20.3×10^6 cell l^{-1} at 6 m depth). The abundance of benthic diatoms increased from 0% to 20% of total species abundance within the sampling period, reaching maximum values on Nov 26 (3.0×10^6 cell l^{-1} at 4.5 m depth; Figure 6a). Principal coordinate analysis (PCO; Figure 6b), on the basis of the Bray–Curtis similarity matrix, showed that the earlier sampling dates tended to cluster together away from the later dates, and 20–25 November clustered separately to 26–29 November; note, however, that there was overlap between the dates, and this was largely a response to high proportions of the diatom *Fragilariopsis obliquecostata* being present on many of the sampling dates.

(**a**)   (**b**)
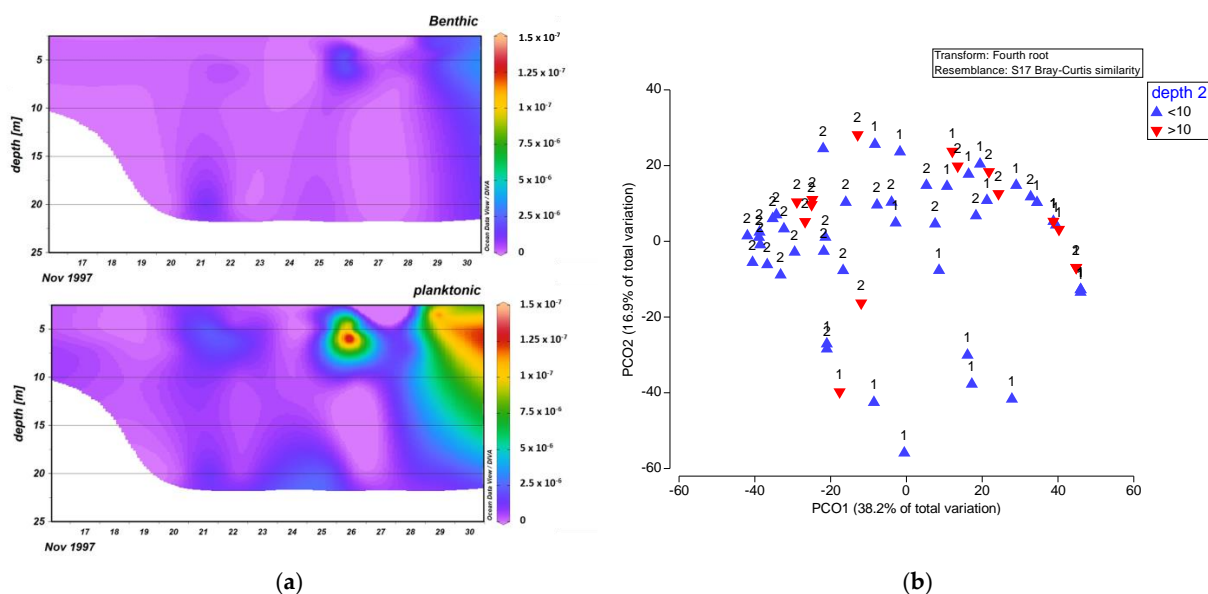
Figure 6. Phytoplankton community, PIPEX Station. (**a**) Benthic and pelagic diatom abundance in cell l^{-1}, daily average. (**b**) Principal coordinate analysis based on counts, labelled as depth < 10 m and > 10 m and dates as phase "1" (up to 22 Nov) and phase "2" (from 25 November).

Table 1. Phytoplankton species sampled at PIPEX station. Size and key habitat are shown.

|	Benthic	Planktonic	Size, μm
Bacillariophyceae			
Berkeleya adeliensis	X		60
Chaetoceros spp.		X	40
Cocconeis sp.	X		21
Cylindrotheca closterium		X	200
Dactyliosolen sp.		X	40
Entomoneis kjellmanii	X		115
Eucampia antarctica		X	110
Fragilariopsis curta		X	40
Fragilariopsis cylindrus		X	35
Fragilariopsis obliquecostata		X	100
Fragilariopsis sublinearis		X	85
Fragilaropsis rhombica		X	40
Melosira sp.		X	30
Navicula jejunoides	X		110
Navicula perminuta	X		15
Navicula spp.	X		85
Nitzschia lecointei	X		100
Nitzschia spp.	X		130
Nitzschia stellata	X		120
Nitzschia taeniiformis	X		140
Odontella weissflogii		X	110
Pleurosigma sp.	X		210
Pseudonitzschia turgiduloides		X	115
Pseudogomphonema kamtschaticum		X	65
Pseudonitzschia lineola		X	200
Pseudonitzschia subcurvata		X	100
Rhizosolenia spp.		X	350
Thalassiosira spp.		X	30
Trigonium sp.		X	220
Prasinophyceae			
Pyramimonas spp.		X	
Prymnesiophyceae			
Phaeocystis sp.		X	
Other flagellates			
Phytoflagellates < 10 μm		X	

3.3. Zooplankton

The zooplankton community was composed of about 20 taxa. Copepods, with their naupliar stages, represented the dominant zooplanktonic group with an overall richness of 14 species (see [60], Table 2 therein). On average, copepods accounted for 47.9 and 50.3%, respectively, of total zooplankton abundance, followed in rank order by invertebrate eggs (1.5%) and tintinnids (0.15%). Copepod total abundances varied significantly across the PIPEX cruise period, with higher values during week I (maximum daily average ≈250 ind m^{-3} on 19 Nov) and a reduction in week II (below 30 ind m^{-3} daily average, after 24 Nov). Total abundances did not vary significantly with depth (ANOVA, Kruskal–Wallis, F = 1.69, p = 0.94) or sampling time (ANOVA, Kruskal–Wallis, F = 2.38, p = 0.12). The under-ice copepod community was characterised by the dominance of the micro-plankton fraction, represented mostly by copepod nauplii, and small sized copepods, with a high occurrence of *Oithona similis*, as copepodites and adults, which contributed to 26 and 15%, respectively, to the total copepod assemblage. In decreasing order of abundance, other common species were *Metridia gerlachei* nauplii and *Oncaea* copepodites, as well as the sea-ice-associated species *Stephos longipes*, *Paralabidocera antarctica*, and *Harpacticus furcifer*. The large mesozooplankton fraction was only occasionally sampled, being represented by the copepods *Calanoides acutus*, *Pleuromamma robusta antarctica*, and *Ctenocalanus citer* (Figure S2).

The naupliar community was dominated by *M. gerlachei* (30%), followed, in decreasing rank of abundance, by *O. similis* (11%), *S. longipes* (8%), and *P. antarctica* (2%) nauplii. Naupliar stages of *S. longipes*, *P. antarctica*, and *M. gerlachei* were more abundant than copepodites and adults of these species, while *O. similis* copepodites and adults outnumbered the naupliar forms. In the *O. similis* population, all developmental stages were widely represented through the water column. On average, naupliar stages showed similar abundances throughout the 20 m water column, attaining higher mean values (10.4 ind m^{-3}), between 4.5 and 5 m depths. Their absolute total abundances ranged from 0.6 to 45.6 ind m^{-3}.

Oithona similis copepodites, represented almost exclusively by CV stage, occurred with higher mean densities (26.2 ind m^{-3}) at 20 m depth. Their numbers ranged from 0.08 to 127.9 ind m^{-3}. They were distributed throughout the water column, showing an increasing abundance with depth. The vertical distribution of *O. similis* adults showed a vertical trend similar to their copepodite stages, but with lower mean abundances (their absolute numbers ranged from 0.2 to 159.8 ind m^{-3}). *Oncaea* copepodites occurred with discrete abundance mean values (4.0 ind m^{-3}), distributed along all sampled water column, representing the 7% of the total copepods. On average, their abundances peaked at 6 m depth with 11.6 ind m^{-3}.

3.3.1. Temporal Distribution

Differences in the zooplankton communities sampled early in the season versus those later in the season were driven more by relative abundances than by taxonomic variation. The temporal variation in four species, which together represented more than 91% of the total abundance (ind m^{-3}), is shown in Figure 7.
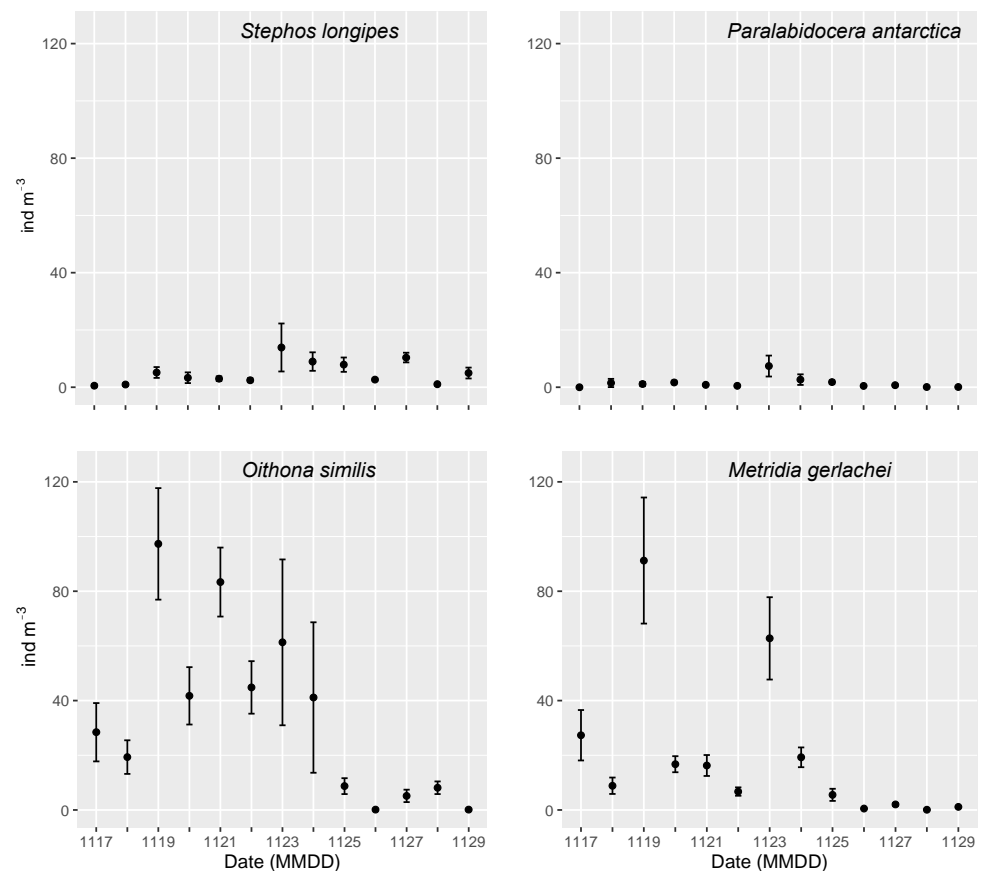
Figure 7. PIPEX 97 cruise, Terra Nova Bay, Antarctica 1997. Trends in abundance (ind m^{-3}) of the main ice-related (*S. longipes*, upper left and *P. antarctica*, upper right) and pelagic (*O. similis*, lower left and *M. gerlachei*, lower right) copepod species. Mean + s.e. values are shown.

The abundances of nauplii oscillated considerably during the sampling period. Abundances of *O. similis* nauplii were higher from 19 to 24 November and decreased towards the end of the sampling period (Figure 8). Copepodite and adult abundances followed a similar trend, attaining peaks of 58.1 ind m^{-3}, entirely linked to CV, and 27.6 ind m^{-3}, on 19 and 23 November, respectively. *M. gerlachei* nauplii reached peaks of densities only on two sampling days (19 and 23 November) almost completely due to NIV; lower numbers occurred at the end of the sampling period. *S. longipes* naupliar abundances fluctuated between all sampling dates, with higher values of NIV on 24 and 25 November, that tended to decrease later when NV became dominant at the end of the sampling period. *P. antarctica* nauplii occurred with higher numbers only on 23 November; the abundances remained more constant during the other sampling dates, decreasing toward the end of the investigation period.
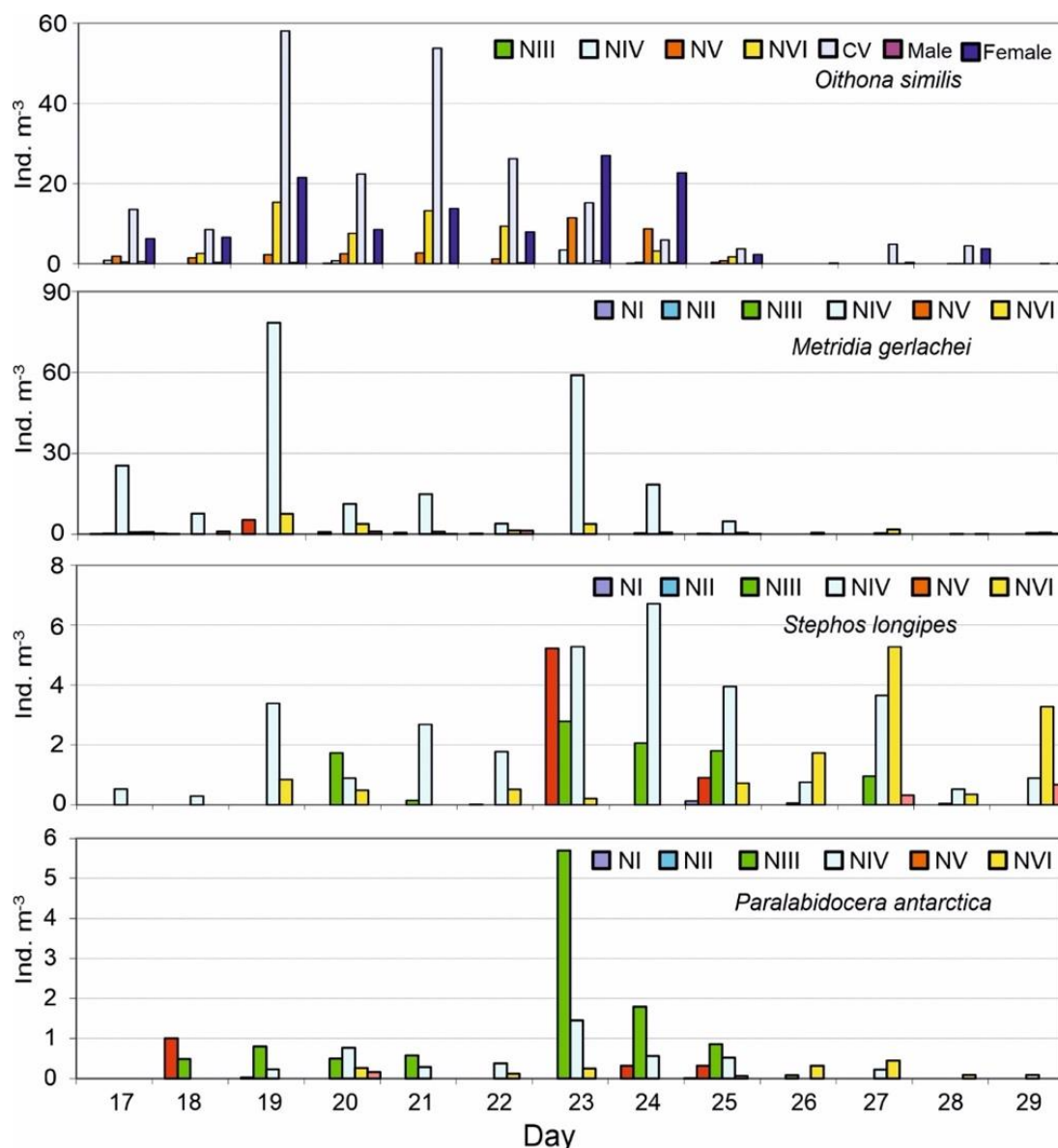
Figure 8. PIPEX 97 cruise, Terra Nova Bay, Antarctica 1997. Average abundance (ind m^{-3}) of the four most representative adult and development stages copepod species throughout the sampling period. Note that naupliar stages NI and NII were not found for the species *O. similis*, which presented conversely copepodites (only CV) and male/female adults.

3.3.2. Copepod Naupliar Vertical Distribution

Naupliar stages of *M. gerlachei* were the dominant developmental form in the copepod assemblage—their total numbers ranged from 0.0 to 213.2 ind m^{-3}. On average, their abundance reached a peak of 24.0 ind m^{-3} at 4.5–5 m depth, then gradually decreased to reach the minimum of 7.3 ind m^{-3} at 20 m depth under sea ice (Figure 9). Naupliar stages of *S. longipes* attained peak in abundances just under the ice at 3.5 m, with maximum mean density of 8.2 ind m^{-3}; they seemed to decrease downward, reaching a minimum of 1.7 ind m^{-3} at 7 m depth and then increased again (up to 6.2 ind m^{-3}) at 10 m under sea ice. However, they occurred throughout the 20 m water column, with absolute abundances ranging from 0.3 to 67.7 ind m^{-3}. *Paralabidocera antarctica* nauplii occurred with higher mean abundances at 3.5 and 4.5–5 m depths (2.1 and 2.3 ind m^{-3}, respectively) and negligible values below these depths. Their absolute abundances ranged from 0.1 to 31.3 ind m^{-3}. Copepodites of this species also occurred, but with very low abundances distributed mostly between 3.5 and 4.5–5 m.
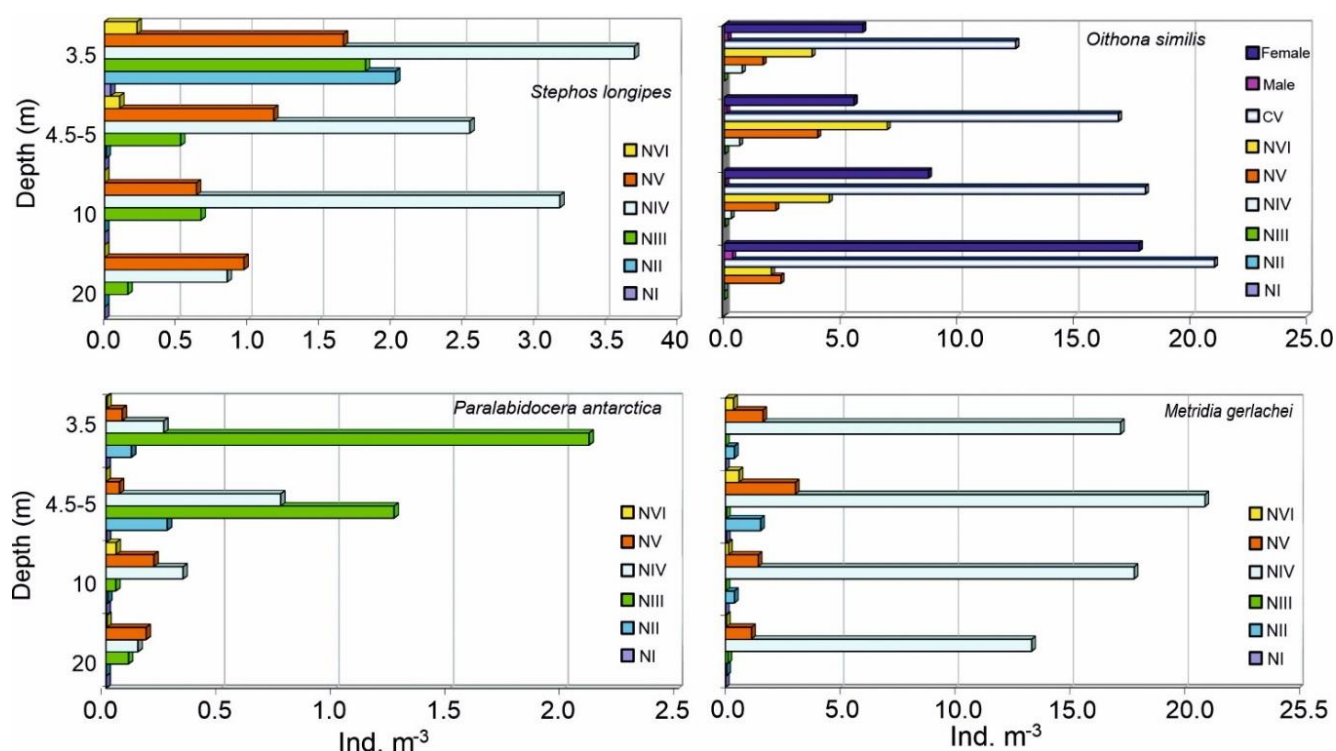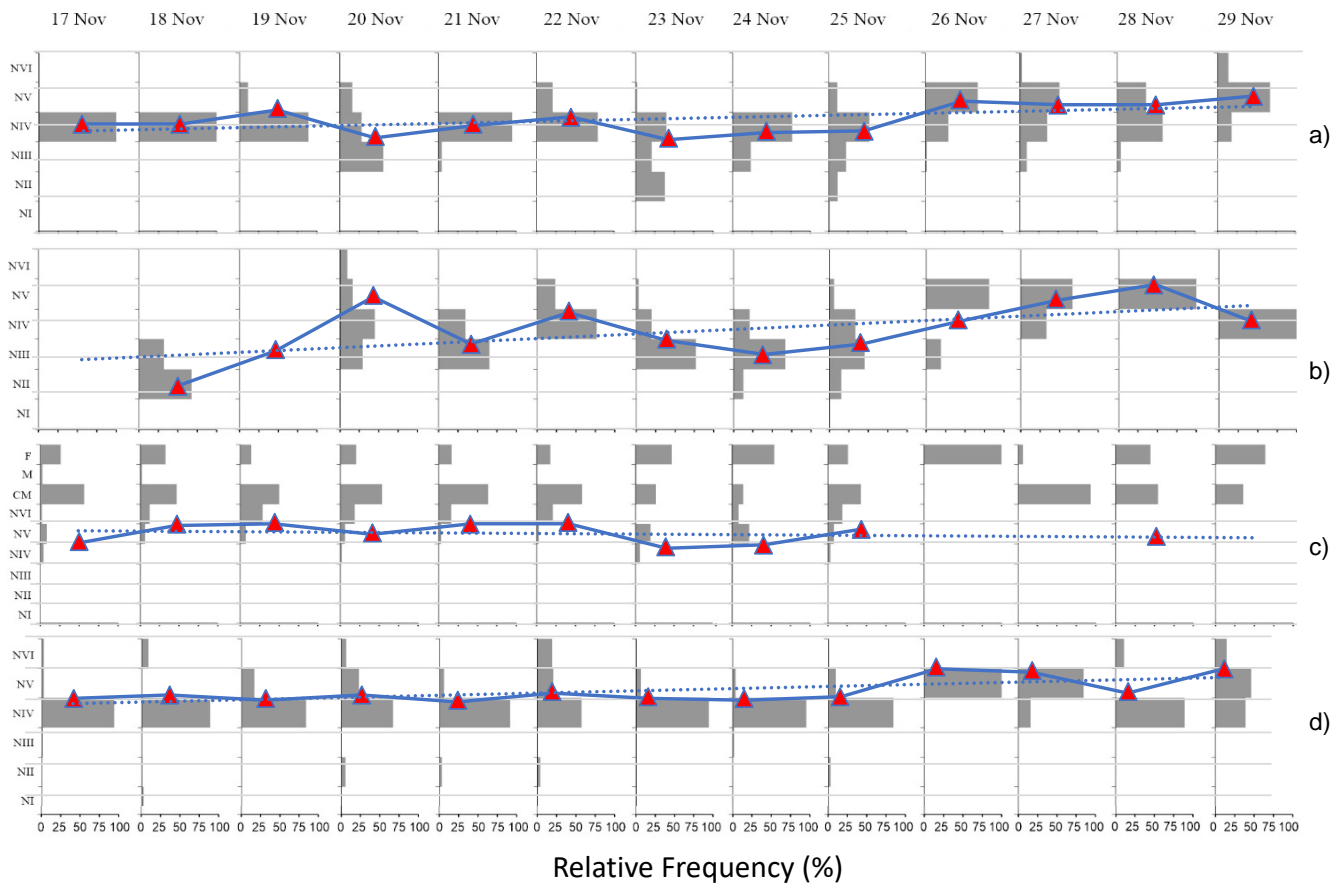

Figure 9. PIPEX 97 cruise, Terra Nova Bay, Antarctica 1997. Average abundance (ind m^{-3}) through the top 20 m of the water column of the four most representative adult and development stages of copepod species throughout the sampling period.

3.3.3. Copepod Naupliar Community Structure

Frequencies of occurrence of the different naupliar stages for each most abundant copepod species are shown in Figure 10. All *S. longipes* naupliar stages co-occurred during the entire study period, but NIV accounted for the main part of the population during all the study period with the exception of the last sampling days, when NV was more dominant. Mean naupliar stage varied between 3.1 on 23 Nov and 4.9 on 29 Nov, with a slight tendency to increase. NIII was the most abundant stage of *P. antarctica* population at the start of the sampling period, whereas, notwithstanding some oscillation, NV become dominant at the end of the study time. The increasing trend of mean naupliar stage, with values ranging from 2.3 to 5.0, was clearer than in the former species. The prevailing composition of *M. gerlachei* was represented by NIV during all the study period, except during the last days, when NV became the most important stage numerically. Its population also showed an increment in the mean naupliar stage, varying from 3.9 to 5.0, through

the study time, even though it was less marked than the previous species. The *O. similis* naupliar population was constituted mostly by stages IV-V, without any significant trend in the naupliar mean stage.

Figure 10. PIPEX 97 cruise, Terra Nova Bay, Antarctica 1997. Frequencies of occurrence and mean naupliar stage (▲) of the most abundant copepod species throughout the sampling period: (**a**) *Stephos longipes*, (**b**) *Paralabidocera antarctica*, (**c**) *Oithona similis*, (**d**) *Metridia gerlachei*. Note that naupliar stages NI and NII were not found for the species *O. similis*, which presented conversely copepodites (only CV) and male/female adults.

4. Discussion

The results of the ROMS simulations highlighted the triggering of the spring phase each year between 1999 and 2013 when the sea ice that completely covered the coastal area of Terra Nova Bay began to melt. Two different behaviours were distinguished throughout the 15-year period, each characterised by (1) the moment when the melting began and (2) the speed at which melting proceeded. There were years when the melting was fast and early (fast-melting years) and others when the melting was late and proceeded more slowly (slow-melting years).

The simulation used was unsuitable for making climatological speculations on a decadal or multi-decadal scale, but nevertheless, the available statistics suggested an equal probability of the two behaviours (53% and 47% for fast-melting and slow-melting years, respectively) that seemed to proceed in alternating batches of 5–7 consecutive years.

The comparisons highlighted that the year of the PIPEX cruise mimicked the behaviour of a slow-melting year. According to the model, the system could then be more dynamic than observed during the PIPEX cruise, even with reference to the first half of November.

Generally, melting was delayed by 10–15 days in slow-melting years compared to fast-melting years, when the ice cover was almost completely absent by the end of November. Consequently, the second half of November is a key fortnight in the Terra Nova Bay region

when the ice and biology are responding rapidly to environmental conditions. The PIPEX 97 cruise took place under a slow-melting scenario, where even in late November, the ice thickness had a median of around 0.65 m and the ocean–ice system close to the coast was less dynamic than it would be during fast-melting years.

Brine channels usually measure between 0.1 and 1000 μm in diameter [78], and the environmental conditions of this habitat are variable in both space and time [79]. The highest weekly temperature fluctuations detected at the air–ice interface during the present study certainly contribute to increasing this variability. Consequently, organisms living within the sea ice are exposed to extremes in temperature and salinity similar to that of intertidal areas [80]. In contrast to the ice interior, the temperature and salinity conditions are rather uniform at the ice–water interface, as confirmed in this study. Since the values of T and S during the second half of November always exceeded the seawater freezing point at 0 m (T ≈ -1.9 °C, S ≈ 35), the observed situation during week II is likely to be attributed to the acceleration of the ongoing melting of the overlying sea ice associated with possible underlying lateral advection of saltier water towards the end of November. At the beginning of our study, the water column exhibited a completely unstructured condition. At the end of the third week, the surface warming became stronger, and, fostered by the pack-ice melting, the pycnocline progressively deepened and generated a mixed layer from 10 to 30 m depth.

This study has highlighted the relationship between biota and ice during the early stages of ice melting in the spring season, providing important information on the timespan and dynamics of both biological and environmental parameters over a short period. Unfortunately, this very short observation window did not allow us to verify the final destiny of the microalgae that were discharged from the ice, although a marked increase in diatoms was evident, essentially in aggregate form, concentrated in the mixed layer between 10 and 30 m. This led us to hypothesise that ice algae must cope with being released into freshening surface water during the melt season, as suggested by Assmy et al. (2013) [81]. Due to their inherent stickiness, the algae are prone to aggregation [82] and subsequent sedimentation [83]. Assmy et al. (2013), during cruises to the Eastern Central Arctic in late summer 2012, observed floating algal aggregates in the melt-water layer below and between melting ice floes of first-year pack-ice [81]. The macroscopic aggregates had a mucous consistency and were dominated by typical ice-associated pennate diatoms. Aggregates maintained buoyancy and accumulated just above a strong pycnocline that separated meltwater and seawater layers.

A major peak in algal sedimentation occurred at the end of the sampling season. The sedimented algae included both ice algae and phytoplankton species. The ice algae did not remain suspended in the plankton biomass, but sedimented rapidly upon release from the ice matrix, as had been observed by Michel et al. (1977) for the Arctic [84]. Both benthic and planktonic species found in our samples were released from the ice, largely coming from the platelet ice. Observations from previous studies carried out on the composition of algae in the Terra Nova Bay sea ice showed that planktonic species were dominant in the platelet ice [85,86], which is consistent with our results indicating that planktonic species dominate in the layers below the sea ice. Given that the increase in algal biomass in platelet ice occurred about three weeks prior to the accumulation of biomass in the bottom ice (e.g., [86,87]), benthic species, which dominate the ice bottom, were not abundant in our samples because they had been trapped in the ice. It is unlikely that these cells were lost during the sampling because they are between 50 and 80 μm in length and form colonies up to a few millimetres long. The evaluation of the sampling effort suggested an extrapolated species richness in the sample was 37 species were pooled (R-Vegan jack-knife 1 estimator, [88]), which suggests that diatom richness was underestimated about 15%. The fact that diatoms were likely underestimated suggests that particular conditions (e.g., lateral inputs of species) may drive an "enrichment" of the diatom community.

During the PIPEX project, pennate diatoms were the dominant taxonomic group of the sympagic microbial communities [86,87]. In particular, the benthic *Amphiprora kufferathii*

and *Nitzschia* species were the most abundant species within the bottom sympagic flora, while the platelet assemblage was mainly pelagic (e.g., *Fragilariopsis nana*). The species belonging to the genus *Fragilariopsis* dominated the pelagic species in our samples, which is consistent with other findings [86,89–91]. The persistence and dominance of *Fragilariopsis obliquecostata* is due to its size, because this species is the largest of the *Fragilariopsis* species. *Phaeocystis antarctica* was recorded in the water below the ice layer, but its abundance has likely been underestimated because single cells (about 5 μm in size) would have been lost by sampling with the 100 μm mesh net.

Our results show that the benthic algae sampled from the water column by the MicroNESS increased slightly with time, due to the dissolution of the land fast ice. The microalgae accumulating at the bottom horizon of the landfast ice follow different pathways. Benthic species do not contribute to the late spring phytoplankton blooms, and hence their high biomass in the bottom ice layer becomes an important food source for both pelagic and benthic food webs. In contrast, planktonic species of the platelet-ice layer are found in high concentrations in ice-free waters [91], showing that this particular ice type constitutes an incubator for the late spring phytoplankton bloom in Terra Nova Bay [86]. Taxonomic composition of the two mixed groups suggests two types of connection between the ice–water interface and the water column, i.e., before the phytoplankton bloom, there was seeding of the water column by ice algae and, during ice melt, interfacial algae contributed to the water column communities that were otherwise typically phytoplankton, as already previously observed [92]. Overall, the phytoplankton community underwent a succession from pennate to centric diatoms. The bulk of the bottom ice carbon biomass was readily exported to the water column through direct sinking (75% of ice export) [83]. These results stress that the main flow of organic carbon at the ice–water interface was through sedimentation of ice algae and suggest that food web interactions within the ice do not influence the availability of ice algae to pelagic grazers in seasonally ice-covered areas. Vertical flux and sedimentation of ice algal material will transfer energy to pelagic and benthic ecosystems [32,93,94]. The sinking rates increased seasonally (0.4–2.7 m d^{-1}), which enhanced accessibility of ice algal cells to the pelagic grazers [92].

In this sector of the Southern Ocean, the metazoan community associated with the annual sea ice is widely dominated by two copepod species, the calanoid *S. longipes* and the harpacticoid *Harpacticus furcifer*, representing together about 90% of the entire zooplankton community at Terra Nova Bay [94]. Later, despite the low species richness and poorly diversified sympagic copepod community, the strong link between some copepod life cycles and annual sea ice growth and melt has been confirmed, supported by the high densities of copepod eggs and naupliar stages of *S. longipes* [45]. Our data on the temporal evolution of both pelagic and ice-associated copepod communities agree with what has already been described for phytoplankton and ice algae. During the late spring of 1997, nauplii dominated the *S. longipes* population (91.6%) and occurred in extremely high concentrations in the lowermost part of the annual sea ice cores, associated with high chlorophyll *a* and phaeopigment levels, while the concentrations, essentially adult specimens, were very low in the platelet layer, and no naupliar stages were found in the water column [45]. Similar results have also been reported [10], supporting the *S. longipes* life cycle strategy already hypothesised [53].

Additionally, differences in sympagic copepod assemblages between Weddell and Ross Seas were observed by sampling ice cores [45]. These species differ markedly in their geographical distribution as well as in their life cycle strategies: the harpacticoid *Drescheriella glacialis* is a dominant sympagic species in most geographical regions and probably has a circum-Antarctic distribution [43,46,55,95]. It appears to spend most of its life in the sea ice [72,95]. Similarly to *D. glacialis*, *S. longipes* has a circum-Antarctic distribution but is more abundant in the Atlantic and Pacific sectors than in the East Indian sector [43,46,53]. Its life cycle seems to be strongly coupled with the annual growth and melting cycle of the sea ice. High abundances of *S. longipes* occur in sea ice during autumn, winter, and spring but are low during the summer when this species is most

abundant in the surface waters [53]. However, in degraded summer ice containing many gaps and empty spaces, *S. longipes* remains in the ice even during summer [43,49,55,96]. *Paralabidocera antarctica* is found mostly in the Indian Ocean where it occurs in the sea ice for most of the year, except in summer, when it concentrates just below the ice (e.g., [51]). To support this hypothesis, there was a decrease in abundance of *O. similis*, *M. gerlachei*, and *P. antarctica* naupliar stages, which lasted from the first to the second week of sampling.

Finally, it is suggested that the PIPEX data and findings be re-considered in future work with a twofold significance: on the one hand, they describe the state of the plankton community at Terra Nova Bay about 25 years ago, and on the other hand, they describe the evolution of the community at the onset of the ice melting process.

Supplementary Materials: The following supporting information can be downloaded at https://www.mdpi.com/article/10.3390/d14060425/s1, Figure S1: The sampling scheme during the PIPEX campaign (17–29 November 1997) in Terra Nova Bay, Antarctica. Overall, 96 tows were performed with MICRONESS at different depths: red dots in-dicate afternoon tows (38), blue dots indicate morning tows (30) and green dots indicate morning and afternoon tows (28). Figure S2: Terra Nova Bay, Antarctica, November 1997. Average per-centage of copepod community structure throughout the sampling period (N = nauplii). Table S1: Sampling routes, at station 5t, of the MicroNESS mounted on "Romeo" ROV. Mouth, 13 cm × 27 cm; mouth area, 0.0351 m^2; 100-μm mesh net; medium speed, 35 cm s^{-1}.

Author Contributions: A.G., A.B. (Alessandro Bergamasco) and L.G. conceptualised the study and jointly wrote the article; A.G., M.S., M.G. and L.G., performed the field/lab analyses and taxonomic identifications; A.B. (Andrea Bergamasco) and A.B. (Alessandro Bergamasco) processed the model dataset; A.B., C.K.W. and K.M.S. reviewed the manuscript; L.G., dealt with funding and management. All authors have read and agreed to the published version of the manuscript.

Institutional Review Board Statement: Not applicable.

Data Availability Statement: The data presented in this study are available on request from the corresponding author.

Conflicts of Interest: The authors declare no conflict of interest.

References

1. Eayrs, C.; Holland, D.; Francis, D.; Wagner, T.; Kumar, R.; Li, X. Understanding the Seasonal Cycle of Antarctic Sea Ice Extent in the Context of Longer-Term Variability. *Rev. Geophys.* **2019**, *57*, 1037–1064. [CrossRef]
2. Parkinson, C.L. A 40-y record reveals gradual Antarctic sea ice increases followed by decreases at rates far exceeding the rates seen in the Arctic. *Proc. Natl. Acad. Sci. USA* **2019**, *116*, 14414–14423. [CrossRef] [PubMed]
3. Arrigo, K.R.; Worthen, D.L.; Lizotte, M.P.; Dixon, P.; Dieckmann, G. Primary Production in Antarctic Sea Ice. *Science* **1997**, *276*, 394–397. [CrossRef]
4. Lizotte, M.P. The contributions of sea ice algae to Antarctic marine primary production. *Am. Zool.* **2001**, *41*, 57–73. [CrossRef]
5. Arrigo, K.R. Primary production in sea ice. In *Sea Ice: An Introduction to Its Physics, Chemistry, Biology and Geology*; Thomas, D.N., Dieckmann, G.S., Eds.; Blackwell Science: London, UK, 2003; pp. 143–183.
6. Günther, S.; George, K.H.; Gleitz, M. High sympagic metazoan abundance in platelet layers at Drescher Inlet, Weddell Sea, Antarctica. *Polar Biol.* **1999**, *22*, 82–89. [CrossRef]
7. McMINN, A.; Ashworth, C.; Ryan, K. Growth and Productivity of Antarctic Sea Ice Algae under PAR and UV Irradiances. *Bot. Mar.* **1999**, *42*, 401–407. [CrossRef]
8. Guglielmo, L.; Carrada, G.C.; Catalano, G.; Dell'Anno, A.; Fabiano, M.; Lazzara, L.; Mangoni, O.; Pusceddu, A.; Saggiomo, V. Structural and functional properties of sympagic communities in the annual sea ice at Terra Nova Bay (Ross Sea, Antarctica). *Polar Biol.* **2000**, *23*, 137–146. [CrossRef]

9.   Thomas, D.; Kattner, G.; Engbrodt, R.; Giannelli, V.; Kennedy, H.; Haas, C.; Dieckmann, G.S. Dissolved organic matter in Antarctic sea ice. *Ann. Glaciol.* **2001**, *33*, 297–303. [CrossRef]

10. Kurbjeweit, F.; Gradinger, R.; Weissenberger, J. The life cycle of Stephos longipes - an example for cryopelagic coupling in the Weddell Sea (Antarctica). *Mar. Ecol. Prog. Ser.* **1993**, *98*, 255–262. [CrossRef]

11. Werner, I.; Auel, H.; Kiko, R. Occurrence of *Anonyx sarsi* (Amphipoda: Lysianassidae) below Arctic pack ice—an example for cryo-benthic coupling? *Polar Biol.* **2004**, *27*, 474–481. [CrossRef]

12. Lovvorn, J.R.; Cooper, L.; Brooks, M.L.; De Ruyck, C.C.; Bump, J.K.; Grebmeier, J. Organic matter pathways to zooplankton and benthos under pack ice in late winter and open water in late summer in the north-central Bering Sea. *Mar. Ecol. Prog. Ser.* **2005**, *291*, 135–150. [CrossRef]

13. Michels, J.; Dieckmann, G.S.; Thomas, D.; Schnack-Schiel, S.B.; Krell, A.; Assmy, P.; Kennedy, H.; Papadimitriou, S.; Cisewski, B. Short-term biogenic particle flux under late spring sea ice in the western Weddell Sea. *Deep Sea Res. Part II Top. Stud. Oceanogr.* **2008**, *55*, 1024–1039. [CrossRef]

14. Fischer, G.; Fütterer, D.; Gersonde, R.; Honjo, S.; Ostermann, D.; Wefer, G. Seasonal variability of particle flux in the Weddell Sea and its relation to ice cover. *Nature* **1988**, *335*, 426–428. [CrossRef]

15. Leventer, A.; Dunbar, R.B. Factors influencing the distribution of diatoms and other algae in the Ross Sea. *J. Geophys. Res. Earth Surf.* **1996**, *101*, 18489–18500. [CrossRef]

16. Fabiano, M.; Pusceddu, A. Total and hydrolizable particulate organic matter (carbohydrates, proteins and lipids) at a coastal station in Terra Nova Bay (Ross Sea, Antarctica). *Polar Biol.* **1998**, *19*, 125–132. [CrossRef]

17. Pusceddu, A.; Dell'Anno, A.; Fabiano, M. Organic matter composition in coastal sediments at Terra Nova Bay (Ross Sea) during summer 1995. *Polar Biol.* **2000**, *23*, 288–293. [CrossRef]

18. Gordon, A.L.; Padman, L.; Bergamasco, A. Southern Ocean shelf slope exchange. *Deep Sea Res. Part II Top. Stud. Oceanogr.* **2009**, *56*, 775–777. [CrossRef]

19. Orsi, A.H.; Wiederwohl, C.L. A recount of Ross Sea waters. *Deep Sea Res. Part II Top. Stud. Oceanogr.* **2009**, *56*, 778–795. [CrossRef]

20. Dinniman, M.S.; Klinck, J.M.; Smith, W.O., Jr. Cross-shelf exchange in a model of the Ross Sea circulation and biogeochemistry. *Deep-Sea Res. II* **2003**, *50*, 3103–3120. [CrossRef]

21. Bergamasco, A.; Defendi, V.; Budillon, G.; Spezie, G. Downslope flow observations near Cape Adare shelf-break. *Antarct. Sci.* **2004**, *16*, 199–204. [CrossRef]

22. Budillon, G.; Spezie, G. Thermoaline structure and variability in the Terra Nova Bay polynya, Ross Sea. *Antarct. Sci.* **2000**, *12*, 493–508. [CrossRef]

23. Fusco, G.; Budillon, G.; Spezie, G. Surface heat fluxes and thermoaline variability in the Ross Sea and in Terra Nova Bay polynya. *Cont. Shelf Res.* **2009**, *29*, 1887–1895. [CrossRef]

24. Hecq, J.H.; Brasseur, P.; Goffart, A.; Lacroix, G.; Guglielmo, L. Modelling approach of the planktonic vertical structure in deep Austral Ocean. The example of the Ross Sea ecosystem. In *Progress in Belgian Oceanographic Research, Proceedings of the annual workshop on Belgian Oceanographic Research*; Royal Academy of Belgium: Brussels, Belgium, 1993; pp. 235–250.

25. Hecq, J.H.; Guglielmo, L.; Goffart, A.; Catalano, G.; Goosse, H. A modeling approach to the Ross Sea plankton ecosystem. In *Ross Sea Ecology: Italiantartide Expeditions (1987-95)*; Faranda, F.M., Guglielmo, L., Ianora, A., Eds.; Springer: Berlin/Heidelberg, Germany, 2000; pp. 395–411.

26. Smith, W.O., Jr.; Nelson, D.M. Phytoplankton bloom produced by a receding ice edge in the Ross Sea: Spatial coherence with the density field. *Science* **1985**, *227*, 163–166. [CrossRef] [PubMed]

27. Nelson, D.M.; Smith, W.O. Phytoplankton bloom dynamics of the western Ross Sea ice edge—II. Mesoscale cycling of nitrogen and silicon. *Deep Sea Res. Part A. Oceanogr. Res. Pap.* **1986**, *33*, 1389–1412. [CrossRef]

28. Smetacek, V.; Scharek, R.; Gordon, L.I.; Eicken, H.; Fahrbach, E.; Rohardt, G.; Moore, S. Early spring phytoplankton blooms in ice platelet layers of the southern Weddell Sea, Antarctica. *Deep Sea Res. Part A. Oceanogr. Res. Pap.* **1992**, *39*, 153–168. [CrossRef]

29. Fabiano, M.; Povero, P.; Danovaro, R. Distribution and composition of particulate organic matter in the Ross Sea (Antarctica). *Polar Biol.* **1993**, *13*, 525–533. [CrossRef]

30. Brierley, A.S.; Thomas, D.N. Ecology of Southern Ocean pack ice. *Adv. Mar. Biol.* **2002**, *43*, 171–276. [CrossRef] [PubMed]

31. Pusceddu, A.; Dell'Anno, A.; Vezzulli, L.; Fabiano, M.; Saggiomo, V.; Cozzi, S.; Catalano, G.; Guglielmo, L. Microbial loop malfunctioning in the annual sea ice at Terra Nova Bay (Antarctica). *Polar Biol.* **2008**, *32*, 337–346. [CrossRef]

32. Cau, A.; Ennas, C.; Moccia, D.; Mangoni, O.; Bolinesi, F.; Saggiomo, M.; Granata, A.; Guglielmo, L.; Swadling, K.M.; Pusceddu, A. Particulate organic matter release below melting sea ice (Terra Nova Bay, Ross Sea, Antarctica): Possible relationships with zooplankton. *J. Mar. Syst.* **2021**, *217*, 103510. [CrossRef]

33. Garrison, D.L.; Sullivan, C.W.; Ackley, S.F. Sea Ice Microbial Communities in Antarctica. *BioScience* **1986**, *36*, 243–250. [CrossRef]

34. Garrison, D.L. Antarctic Sea Ice Biota. *Am. Zool.* **1991**, *31*, 17–34. [CrossRef]

35. Dieckmann, G.S.; Eicken, H.; Haas, C.; Garrison, D.L.; Gleitz, M.; Lange, M.; Nöthig, E.-M.; Spindler, M.; Sullivan, C.W.; Thomas, D.N.; et al. A compilation of data on sea ice algal standing crop from the Bellinghausen, Amundsen and Weddell Seas from 1983–1994. In *Antarctic Sea Ice: Biological Processes, Interactions and Variability*; Antarctic Research Series; Lizotte, M.P., Arrigo, K.R., Eds.; American Geophysical Union: Washington, DC, USA, 1998; pp. 85–92.

36. Gleitz, M.; Bartsch, A.; Dieckmann, G.S.; Eicken, H.S. Composition and succession of sea ice diatom assemblages in the eastern and southern Weddell Sea, Antarctica. *Antarct. Res. Ser.* **1998**, 107–120.

37. Vacchi, M.; LA Mesa, M.; Dalu, M.; Macdonald, J. Early life stages in the life cycle of Antarctic silverfish, Pleuragramma antarcticum in Terra Nova Bay, Ross Sea. *Antarct. Sci.* **2004**, *16*, 299–305. [CrossRef]
38. Granata, A.; Zagami, G.; Vacchi, M.; Guglielmo, L. Summer and spring trophic niche of larval and juvenile Pleuragramma antarcticum in the Western Ross Sea, Antarctica. *Polar Biol.* **2008**, *32*, 369–382. [CrossRef]
39. Archer, S.; Leakey, R.; Burkill, P.; Sleigh, M. Microbial dynamics in coastal waters of East Antarctica:herbivory by heterotrophic dinoflagellates. *Mar. Ecol. Prog. Ser.* **1996**, *139*, 239–255. [CrossRef]
40. Delille, D.; Rosiers, C. Seasonal changes of Antarctic marine bacterioplankton and sea ice bacterial assemblages. *Polar Biol.* **1996**, *16*, 27–34. [CrossRef]
41. Spindler, M.; Dieckmann, G.S.; Lange, M.A. Seasonal and geographic variations in sea ice community structure of the Weddell Sea, Antarctica. In *Antarctic Ecosystems, Ecological Change and Conservation*; Kerry, K.R., Hempel, G., Eds.; Springer: Berlin/Heidelberg, Germany, 1990; pp. 129–135.
42. Swadling, K.M.; Gibson, J.A.; Ritz, D.A.; Nichols, P.D. Horizontal patchiness in sympagic organisms of the Antarctic fast ice. *Antarct. Sci.* **1997**, *9*, 399–406. [CrossRef]
43. Schnack-Schiel, S.B.; Thomas, D.N.; Dahms, H.-U.; Haas, C.; Mizdalski, E. Copepods in Antarctic sea ice. In Antarctic sea ice: Biological processes, interactions and variability. *Antarct. Res. Ser.* **1998**, *73*, 173–182.
44. Gradinger, R. Integrated abundance and biomass of sympagic meiofauna in Arctic and Antarctic pack ice. *Polar Biol.* **1999**, *22*, 169–177. [CrossRef]
45. Guglielmo, L.; Zagami, G.; Saggiomo, V.; Catalano, G.; Granata, A. Copepods in spring annual sea ice at Terra Nova Bay (Ross Sea, Antarctica). *Polar Biol.* **2006**, *30*, 747–758. [CrossRef]
46. Swadling, K.M.; McPhee, A.D.; McMinn, A. Spatial distribution of copepods in fast ice of eastern Antarctica. *Polar Biosci.* **2000**, *13*, 55–65.
47. Schnack-Schiel, S.B.; Dieckmann, G.S.; Gradinger, R.; Spindler, M.; Melnikov, I.A.; Thomas, D.N. Meiofauna in sea ice of the Weddell Sea (Antarctica). *Polar Biol.* **2002**, 180–184.
48. Schnack-Schiel, S.B.; Michels, J.; Mizdalski, E.; Schodlok, M.P.; Schröder, M. Composition and community structure of zooplankton in the sea ice-covered western Weddell Sea in spring 2004—with emphasis on calanoid copepods. *Deep Sea Res. Part II Top. Stud. Oceanogr.* **2008**, *55*, 1040–1055. [CrossRef]
49. Schnack-Schiel, S.B.; Haas, C.; Michels, J.; Mizdalski, E.; Schünemann, H.; Steffens, M.; Thomas, D. Copepods in sea ice of the western Weddell Sea during austral spring 2004. *Deep Sea Res. Part II Top. Stud. Oceanogr.* **2008**, *55*, 1056–1067. [CrossRef]
50. Kramer, M.; Swadling, K.M.; Meiners, K.M.; Kiko, R.; Scheltz, A.; Nicolaus, M.; Werner, I. Antarctic sympagic meiofauna in winter: Comparing diversity, abundance and biomass between perennially and seasonally ice-covered regions. *Deep Sea Res. Part II Top. Stud. Oceanogr.* **2011**, *58*, 1062–1074. [CrossRef]
51. Tanimura, A.; Hoshiai, T.; Fukuchi, M. The life cycle strategy of the ice-associated copepod, *Paralabidocera antarctica* (Calanoida, Copepoda), at Syowa Station, Antarctica. *Antarct. Sci.* **1996**, *8*, 257–266. [CrossRef]
52. Swadling, K.M. Population structure of two Antarctic ice associated copepods, *Drescheriella glacialis* and *Paralabidocera antarctica*, in winter sea ice. *Mar. Biol.* **2001**, *139*, 597–603.
53. Schnack-Schiel, S.B.; Thomas, D.; Dieckmann, G.S.; Eicken, H.; Gradinger, R.; Spindler, M.; Weissenberger, J.; Mizdalski, E.; Beyer, K. Life cycle strategy of the Antarctic calanoid copepod Stephos longipes. *Prog. Oceanogr.* **1995**, *36*, 45–75. [CrossRef]
54. Schnack-Schiel, S.B. The macrobiology of sea ice. In *Sea Ice: An Introduction to Its Physics, Chemistry, Biology and Geology*; Thomas, D.N., Dieckmann, G.S., Eds.; Blackwell Science: London, UK, 2003; pp. 211–239.
55. Schnack-Schiel, S.B.; Thomas, D.N.; Haas, C.; Dieckmann, G.S.; Alheit, R. The occurrence of the copepods *Stephos longipes* (Calanoida) and *Drescheriella glacialis* (Harpacticoida) in summer sea ice in the Weddell Sea, Antarctica. *Antarct. Sci.* **2001**, *13*, 150–157. [CrossRef]
56. Arndt, C.E.; Swadling, K.M. Crustacea in Arctic and Antarctic Sea Ice: Distribution, Diet and Life History Strategies. *Adv. Mar. Biol.* **2006**, *51*, 197–315.
57. Saggiomo, V.; Carrada, G.C.; Mangoni, O.; Marino, D.; Ribera d'Alcalà, A.M. Physiological and ecological aspects of primary production in the Ross Sea. In *Ross Sea Ecology: Italiantartide Expeditions (1987-95)*; Faranda, F.M., Guglielmo, L., Ianora, A., Eds.; Springer: Berlin/Heidelberg, Germany, 2000; pp. 247–258.
58. Mangoni, O.; Modigh, M.; Conversano, F.; Carrada, G.C.; Saggiomo, V. Effects of summer ice coverage on phytoplankton assemblages in the Ross Sea, Antarctica. *Deep-Sea Res. I* **2004**, *51*, 1601–1617. [CrossRef]
59. Wiebe, P.H.; Benfield, M.C. From the Hensen net toward four-dimensional biological oceanography. *Prog. Oceanogr.* **2003**, *56*, 7–136. [CrossRef]
60. Guglielmo, L.; Arena, G.; Brugnano, C.; Guglielmo, R.; Granata, A.; Minutoli, R.; Sitran, R.; Zagami, G.; Bergamasco, A. MicroNESS: An innovative opening–closing multinet for under pack-ice zooplankton sampling. *Polar Biol.* **2015**, *38*, 2035–2046. [CrossRef]
61. Dinniman, M.S.; Klinck, J.M.; Hofmann, E.E.; Smith, W.O., Jr. Effects of Projected Changes in Wind, Atmospheric Temperature, and Freshwater Inflow on the Ross Sea. *J. Clim.* **2018**, *31*, 1619–1635. [CrossRef]
62. Lund, J.W.G.; Kipling, C.; Le Cren, E.D. The inverted microscope method of estimating algal numbers and the statistical basis of estimations by counting. *Hydrobiologia* **1958**, *11*, 143–170. [CrossRef]
63. Utermohl, H. Zur Vervollkommnung der Quantitativen Phytoplankton-Methodik. *SIL Commun.* **1958**, *9*, 1–38. [CrossRef]
64. Medlin, L.K.; Priddle, J. *Polar Marine Diatoms*; British Antarctic Survey: Cambridge, UK, 1990; pp. 1–214.

65. Hasle, G.R.; Syvertsen, E.E. Marine diatoms. In *Identifying Marine Phytoplankton*; Tomas, C.R., Ed.; Academic Press: San Diego, CA, USA, 1997; pp. 5–385.

66. Scott, F.J.; Thomas, D.P. Diatoms. In *Antarctic Marine Protists*; Scott, F.J., Marchant, H.J., Eds.; Australian Biological Resources Study: Canberra, Australia; Australian Antarctic Division: Hobart, Australia, 2005; pp. 13–201.

67. Zingone, A.; Totti, C.; Sarno, D.; Cabrini, M.; Caroppo, C.; Giacobbe, M.G.; Lugliè, A.; Nuccio, C.; Socal, G. Fitoplancton: Metodiche di analisi quali-quantitativa. In *Metodologie di Studio del Plancton Marino*; Socal, G., Buttino, I., Cabrini, M., Mangoni, O., Penna, A., Totti, C., Eds.; Manuali E Linee Guida 56 ISPRA SIBM: Roma, Italy, 2010; pp. 204–228.

68. Giesbrecht, W. Zoologie: Copepoden. In *Expédition Antarctique Belge. Résultats du Voyage du S.Y. Belgica en 1897–1898–1899. Rapports Scientifiques (1901–1913)*; Gerlache de Gomery, A., Ed.; Imprimerie J.-E. Buschmann: Anvers, Belgium, 1902; pp. 1–49.

69. Lang, K. Marine Harpacticiden von der Campbell-Insel und einigenanderen südlichen Inseln. *Acta Univ. Lund. New Ser. 2* **1934**, *30*, 1–56.

70. Lang, K. Monographie der Harpacticiden. Hakan Ohlssons Boktryckeri, Lund, Almqvist & Wiksells Boktryckeri Ab, Uppsala. 1948, p. 1682. Available online: https://www.marinespecies.org/copepoda/aphia.php?p=sourcedetails&id=401 (accessed on 20 April 2022).

71. Dahms, H.-U. Postembryonic development of Drescheriella glacialis Dahms & Dieckmann (Copepoda, Harpacticoida) reared in the laboratory. *Polar Biol.* **1987**, *8*, 81–93.

72. Dahms, H.U.; Dieckmann, G.S. *Drescheriella glacialis* gen. nov., sp. nov. (Copepoda, Harpacticoida) from the Antarctic sea ice. *Polar Biol.* **1987**, *7*, 329–337. [CrossRef]

73. Dahms, H.U.; Schminke, H.K. Sea ice inhabiting Harpacticoida (Crustacea, Copepoda) of the Weddell Sea (Antarctica). *Biologie* **1992**, *62*, 91–123.

74. Costanzo, G.; Zagami, G.; Granata, A.; Crescenti, N. Naupliar Development of Stephos Longipes (Copepoda: Calanoida) from the Annual Sea Ice of Terra Nova Bay, Antarctica. *J. Crustac. Biol.* **2002**, *22*, 855–860. [CrossRef]

75. Huntley, M.; Escritor, F. Dynamics of Calanoides acutus (Copepoda: Calanoida) in Antarctic coastal waters. *Deep Sea Res. Part A. Oceanogr. Res. Pap.* **1991**, *38*, 1145–1167. [CrossRef]

76. Legendre, P.; Legendre, L. *Numerical Ecology*; Elsevier: Amsterdam, The Netherlands, 1998; pp. 1–852.

77. Oksanen, J.; Blanchet, F.G.; Kindt, R.; Legendre, P.; Minchin, P.R.; O'Hara, R.B.; Simpson, G.L.; Solymos, P.; Stevens, M.H.H.; Wagner, H. Vegan: Community Ecology Package, 2014, R Package Version 2.2-0. Available online: http://CRAN.Rproject.org/package=vegan (accessed on 20 April 2022).

78. Krembs, C.; Gradinger, R.; Spindler, M. Implications of brine channel geometry and surface area for the interaction of sympagic organisms in Arctic sea ice. *J. Exp. Mar. Biol. Ecol.* **2000**, *243*, 55–80. [CrossRef]

79. Gradinger, R.R. Adaptation of Arctic and Antarctic ice metazoa to their habitat. *Zoology* **2001**, *104*, 339–345. [CrossRef]

80. Brugnano, C.; D'Adamo, R.; Fabbrocini, A.; Granata, A.; Zagami, G. Zooplankton responses to hydrological and trophic variability in a Mediterranean coastal ecosystem (Lesina Lagoon, South Adriatic Sea). *Chem. Ecol.* **2011**, *27*, 461–480. [CrossRef]

81. Assmy, P.; Ehn, J.K.; Fernández-Méndez, M.; Hop, H.; Katlein, C.; Sundfjord, A.; Bluhm, K.; Daase, M.; Engel, A.; Fransson, A.; et al. Floating Ice-Algal Aggregates below Melting Arctic Sea Ice. *PLoS ONE* **2013**, *8*, e76599. [CrossRef] [PubMed]

82. Riebesell, U.; Schloss, I.; Smetacek, V. Aggregation of algae released from melting sea ice: Implications for seeding and sedimentation. *Polar Biol.* **1991**, *11*, 239–248. [CrossRef]

83. Michel, C.; Nielsen, T.; Nozais, C.; Gosselin, M. Significance of sedimentation and grazing by ice micro- and meiofauna for carbon cycling in annual sea ice (northern Baffin Bay). *Aquat. Microb. Ecol.* **2002**, *30*, 57–68. [CrossRef]

84. Michel, C.; Legendre, L.; Taguchi, S. Coexistence of microalgal sedimentation and water column recycling in a seasonally ice-covered ecosystem (Saroma-ko Lagoon, Sea of Okhotsk, Japan). *J. Mar. Res.* **1997**, *11*, 133–148. [CrossRef]

85. Mangoni, O.; Carrada, G.C.; Modigh, M.; Catalano, G.; Saggiomo, V. Photoacclimation in Antarctic bottom ice algae: An experimental approach. *Polar Biol.* **2008**, *32*, 325–335. [CrossRef]

86. Saggiomo, M.; Poulin, M.; Mangoni, O.; Lazzara, L.; De Stefano, M.; Sarno, D.; Zingone, A. Spring-time dynamics of diatom communities in landfast and underlying platelet-ice in Terra Nova Bay, Ross Sea, Antarctica. *J. Mar. Res.* **2017**, *166*, 26–36. [CrossRef]

87. Lazzara, L.; Nardello, I.; Ermanni, C.; Mangoni, O.; Saggiomo, V. Light environment and seasonal dynamics of microalgae in the annual sea ice at Terra Nova Bay, Ross Sea, Antarctica. *Antarct. Sci.* **2007**, *19*, 83–92. [CrossRef]

88. Chao, A. Estimating the Population Size for Capture-Recapture Data with Unequal Catchability. *Biometrics* **1987**, *43*, 783. [CrossRef] [PubMed]

89. Nuccio, C.; Innamorati, M.; Lazzara, L.; Mori, G.; Massi, L. Spatial and temporal distribution of phytoplankton assemblages in the Ross Sea. In *Ross Sea Ecology: Italiantartide Expeditions (1987-95)*; Faranda, F.M., Guglielmo, L., Ianora, A., Eds.; Springer: Berlin/Heidelberg, Germany, 2000; pp. 231–245.

90. Innamorati, M.; Mori, G.; Massi, L.; Lazzara, L.; Nuccio, C. Phytoplankton Biomass Related to Environmental Factors in the Ross Sea. In *Ross Sea Ecology*; Springer: Berlin/Heidelberg, Germany, 2000; pp. 217–230.

91. Mangoni, O.; Saggiomo, M.; Modigh, M.; Catalano, G.; Zingone, A.; Saggiomo, V. The role of platelet ice microalgae in seeding phytoplankton blooms in Terra Nova Bay (Ross Sea, Antarctica): A mesocosm experiment. *Polar Biol.* **2008**, *32*, 311–323. [CrossRef]

92. Michel, C.; Legendre, L.; Therriault, J.C.; Demers, S.; Vandevelde, T. Springtime coupling between ice algal and phytoplankton assemblages in southeastern Hudson Bay, Canadian arctic. *Polar Biol.* **1993**, *13*, 441–449. [CrossRef]

93. Pusceddu, A.; Cattaneo-Vietti, R.; Albertelli, G.; Fabiano, M. Origin, biochemical composition and vertical flux of particulate organic matter under the pack ice in Terra Nova Bay (Ross Sea, Antarctica). *Polar Biol.* **1999**, *22*, 124–132. [CrossRef]

94. Guglielmo, L.; Carrada, G.C.; Catalano, G.; Cozzi, S.; Dell'Anno, A.; Fabiano, M.; Granata, A.; Lazzara, L.; Lorenzelli, R.; Manganaro, A.; et al. Biogeochemistry and algal communities in the annual sea ice at Terra Nova Bay (Ross Sea, Antarctica). *Chem. Ecol.* **2004**, *20*, 43–55. [CrossRef]

95. Dahms, H.U.; Bergmann, M.; Schminke, H.K. Distribution and adaptations of sea ice inhabiting Harpacticoida (Crustacea, Copepoda) of the Weddell Sea (Antarctica). *Mar. Ecol.* **1990**, *11*, 207–226. [CrossRef]

96. Thomas, D.N.; Lara, R.J.; Haas, C.; Schnack-Schiel, S.B.; Dieckmann, G.S.; Kattner, G.; Nöthig, E.-M.; Mizdalski, E. Biological soup within decaying summer sea ice in the Amundsen Sea, Antarctica. In *Antarctic Sea Ice: Biological Processes, Interactions and Variability*; Antarctic Research Series; Lizotte, M.P., Arrigo, K.R., Eds.; American Geophysical Union: Washington, DC, USA, 1998; pp. 161–171.